electronics

MDPI

Article

Wideband and High-Gain Wearable Antenna Array with Specific Absorption Rate Suppression

Haoran Zu [1], Bian Wu [1,*], Peibin Yang [2], Wenhua Li [1] and Jinjin Liu [1]

[1] National Key Laboratory of Antennas and Microwave Technology, Xi'an Key Laboratory of Millimeter Wave and Terahertz Technology, Xidian University, Xi'an 710071, China; zuhr@foxmail.com (H.Z.); whli_2@stu.xidian.edu.cn (W.L.); jinjinliu@stu.xidian.edu.cn (J.L.)
[2] AVIC the First Aircraft Institute, Xi'an 710089, China; y_pb@163.com
* Correspondence: bwu@mail.xidian.edu.cn

Abstract: In this paper, a wideband and high-gain antenna array with specific absorption rate suppression is presented. By adopting the wideband monopole antenna array and the uniplanar compact electromagnetic band gap (UC-EBG) structure, the proposed wearable antenna array can realize a high gain of 11.8–13.6 dBi within the operating band of 4.5–6.5 GHz. The sidelobe level of the proposed wearable antenna array is less than −12 dB, and the cross polarization in the main radiation direction is less than −35 dB. Benefiting from the UC-EBG design, the specific absorption rate is suppressed effectively, guaranteeing the safety of the proposed antenna array to the human body. The proposed antenna array is processed and tested, and the measurement results show good agreement with the simulation results.

Keywords: antenna array; wideband; high gain; specific absorption rate; wearable application

check for updates

Citation: Zu, H.; Wu, B.; Yang, P.; Li, W.; Liu, J. Wideband and High-Gain Wearable Antenna Array with Specific Absorption Rate Suppression. *Electronics* **2021**, *10*, 2056. https://doi.org/10.3390/electronics10172056

Academic Editor: Andrea Randazzo

Received: 7 August 2021
Accepted: 23 August 2021
Published: 26 August 2021

Publisher's Note: MDPI stays neutral with regard to jurisdictional claims in published maps and institutional affiliations.

Copyright: © 2021 by the authors. Licensee MDPI, Basel, Switzerland. This article is an open access article distributed under the terms and conditions of the Creative Commons Attribution (CC BY) license (https://creativecommons.org/licenses/by/4.0/).

1. Introduction

The communication system based on the human-body wireless area network [1] has gradually become a research hotspot due to the wide range of applications, such as human health monitoring [2], on-body wireless communication [3] and telemedicine [4]. Meanwhile, due to the requirements of the on-body working environment, some special performance needs to be satisfied for on-body devices, especially the antennas [5]. The on-body antennas for wearable applications usually need to provide a low profile, high gain, flexibility and wideband. As a result, many works related to the materials [6], design methods [7] and performance [8,9] for wearable antennas have been proposed in the last decades.

In recent years, planar wearable antennas based on various flexible substrates have emerged, which can be roughly divided into the following types: monopole form [10–12], microstrip patch form [13,14], monopole combined with reflective structures such as artificial magnetic conductor (AMC) [15–18] or electromagnetic band gap (EBG) [19–23]. In the case of monopole antennas, the structure is simple and it is easy to realize a wideband design, but there is usually no metal backplane to protect the human body from radiation. The backward radiation of the antenna will lead to a high specific absorption rate (SAR) value, which does not comply with the international electromagnetic radiation safety standards. The microstrip patch form can isolate the human body from the antenna through the metal ground while the bandwidth is narrow, and the movement or deformation of the human body may cause the operating frequency offset and radiation pattern distortion. The combination of the monopole and the reflective structure will enhance the forward radiation, achieving high isolation, thereby significantly reducing the SAR value and the radiation harm caused by the antenna. However, these works mentioned above [10–23] mainly focus on the single wearable antenna, while being committed to balancing the gain, bandwidth and SAR. There are few works reported on the wearable antenna array, not to mention the realization of the wearable antenna array with high gain and wide operating

band, which limits the application of wearable antennas. Ref. [24] has realized the design of a microstrip wearable antenna array with low SAR. Suffering from the disadvantages of microstrip antenna form, the bandwidth of this antenna array is relatively narrow, and the realized gain is relatively low. Therefore, the design of a wearable antenna array taking both bandwidth and high gain into account is still a challenge.

In this paper, an antenna array based on the combination of the monopole antennas and uniplanar compact EBG (UC-EBG) structures is proposed, which has the characteristics of wide band and high gain. Firstly, a wideband flexible monopole antenna is realized by slotting and corner cut. Subsequently, the UC-EBG structure is designed, which is placed under the monopole antenna as a reflector. It can increase the directivity and gain of the antenna, while suppressing the backward radiation, reducing the SAR value to meet international standards. Finally, the four antenna elements are combined with the feeding network to realize the design of a wearable wideband high-gain antenna array. The antenna array can achieve a realized gain of 11.8–13.6 dBi in the range of 4.5–6.5 GHz, the sidelobe level is less than −12 dB and the cross polarization is less than −35 dB for the main radiation direction, showing good potential in on-body communication.

2. Antenna Design

The proposed wearable antenna array utilizes miniaturized wideband monopole elements as radiators, while the UC-EBG structure is loaded below the antenna array. Since the UC-EBG reflecting the backward electromagnetic energy for forward radiation, the antenna directivity and gain can be improved, while guaranteeing the safety of the proposed antenna array to the human body.

2.1. Monopole Antenna and UC-EBG Design

For achieving the wideband and high-gain wearable antenna array with low SAR, the design of the wideband monopole element and UC-EBG structure should be considered.

Figure 1 illustrates the structure of the designed monopole antenna, which is excited by microstrip and the whole dimension is 27.3 mm × 20 mm × 1.1 mm. Since the copper cannot be attached to polydimethylsiloxane (PDMS) by printed circuit board (PCB) process, the substrate consisting of multi-layer flexible dielectric materials is utilized to facilitate the PCB process and satisfy the flexible requirement of the wearable application. The multi-layer dielectric substrate is composed of 0.05 mm-thick polyimide (PI) (dielectric constant 3.5/loss tangent 0.0027), 1 mm-thick PDMS with a dielectric constant of 2.7, loss tangent 0.013. The top and bottom PI layers are coated with copper patterns as depicted in Figure 1a. Figure 1b depicts the top and bottom views of the flexible broadband monopole antenna. Different from the traditional rectangular patch, cutting two triangles at the bottom of the rectangular patch and a set of parallel slots in the top area help to extend the current path and widen the bandwidth of the antenna [25,26]. The specific geometrical dimensions of the proposed monopole antenna are shown in Table 1.

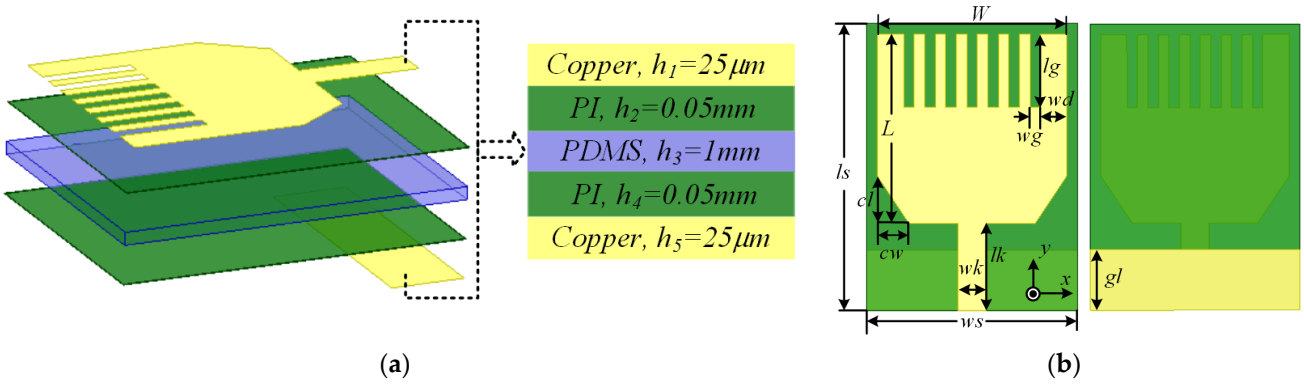

Figure 1. (**a**) Layered graph of the proposed monopole antenna. (**b**) Top view and bottom view of the proposed monopole antenna.

Table 1. Geometrical parameters of the proposed antenna.

Parameter	Value (mm)	Parameter	Value (mm)
W	18	*cl*	4.5
L	18	*cw*	3
lg	7	*ls*	27.3
wg	1	*ws*	20
wd	2.5	*wk*	2.7
gl	5.8	*lk*	8.3

Figure 2a depicts the current distribution of the proposed monopole antenna, which indicates that the slotting and corner cut extend the current path for benefiting the operating bandwidth. Figure 2b plots the reflection coefficient of the monopole antenna with or without slotting and corner cut, which proves the improvement of working bandwidth within 3.4 GHz to 7.9 GHz. The reflection coefficient of the proposed monopole antenna is less than −10 dB, which indicates a good impedance match. Moreover, Figure 3 displays the radiation patterns of the monopole antenna at different frequencies, which proves that the antenna can maintain a stable radiation pattern in a wide working band. Both the impedance and radiation performance demonstrate that the proposed monopole antenna can operate within a wide band from 4 GHz to 7 GHz.

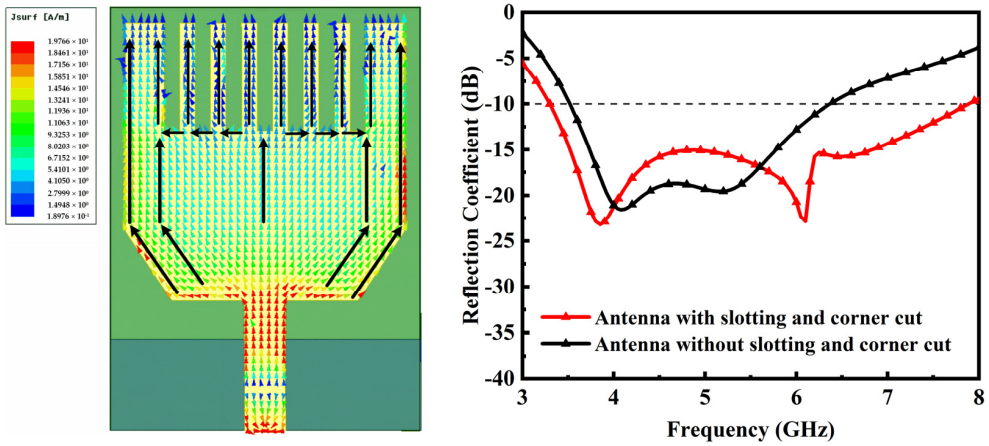

Figure 2. (**a**) The current distribution of the proposed monopole antenna. (**b**) Reflection coefficient of the monopole antenna with or without parallel slots and corner cut.

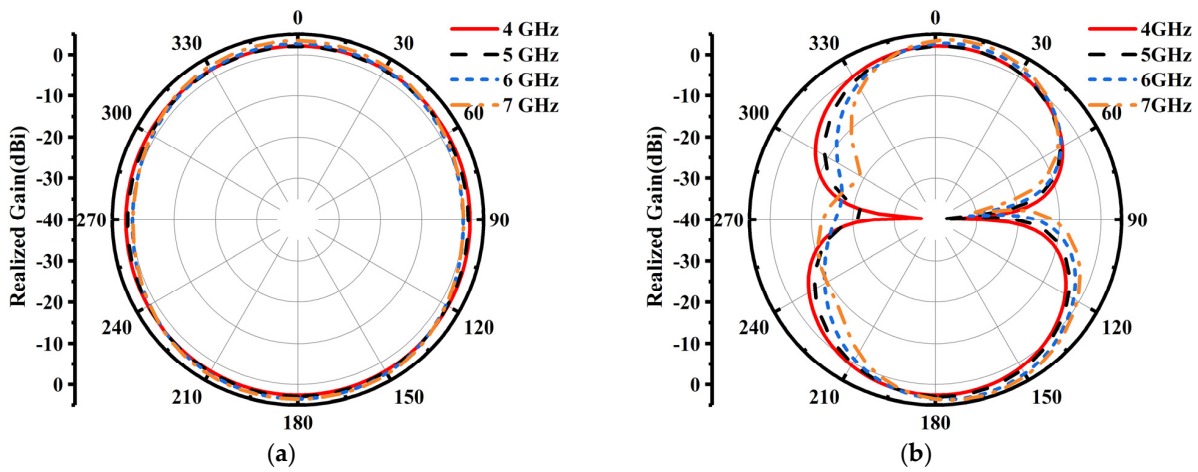

Figure 3. The radiation patterns of the monopole antenna at different frequencies. (**a**) xoz plane. (**b**) yoz plane.

For suppressing the backward radiation to guarantee the safety of the proposed antenna array to the human body and improve the antenna directivity, the UC-EBG structure was utilized to reflect the backward radiation, which was placed below the monopole antenna. To guarantee the wide operating band and offer in-phase reflection, the UC-EBG was designed and is depicted in Figure 4a, and the specific geometrical dimensions are p = 10 mm, $w1$ = 0.2 mm, $l1$ = 2 mm, $w2$ = 0.2 mm, s = 0.17 mm, $p1$ = 4 mm. Figure 4b plots the reflection phase of the proposed UC-EBG. By changing the geometrical dimensions of UC-EBG, the in-phase reflection band can be controlled. As $p1$ = 4 mm, the value of the reflection phase is between −90° and 90° from 4.5 GHz to 6.5 GHz, which can be considered as in-phase reflection.

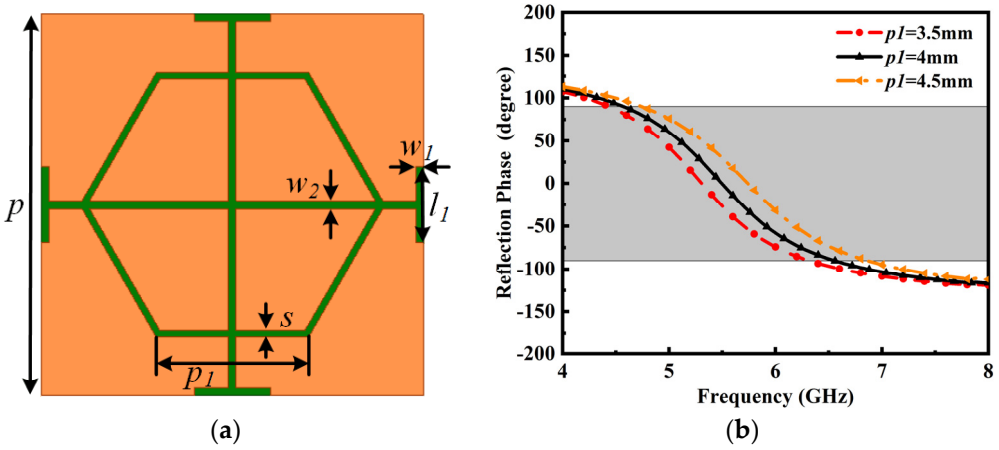

Figure 4. (**a**) Configuration of the proposed UC-EBG. (**b**) Reflection phase of the proposed UC-EBG.

Based on the above analysis, the designed flexible wideband monopole antenna was combined with the UC-EBG structure to form the flexible wearable wideband antenna as shown in Figure 5a. The whole structure is divided into the upper monopole antenna and the lower UC-EBG. The monopole antenna is placed above the UC-EBG structure at H = 4 mm symmetrically along the y-axis. In order to support the monopole antenna above the UC-EBG structure, the propping foam is utilized. The configuration of the monopole antenna with UC-EBG is displayed in Figure 5b.

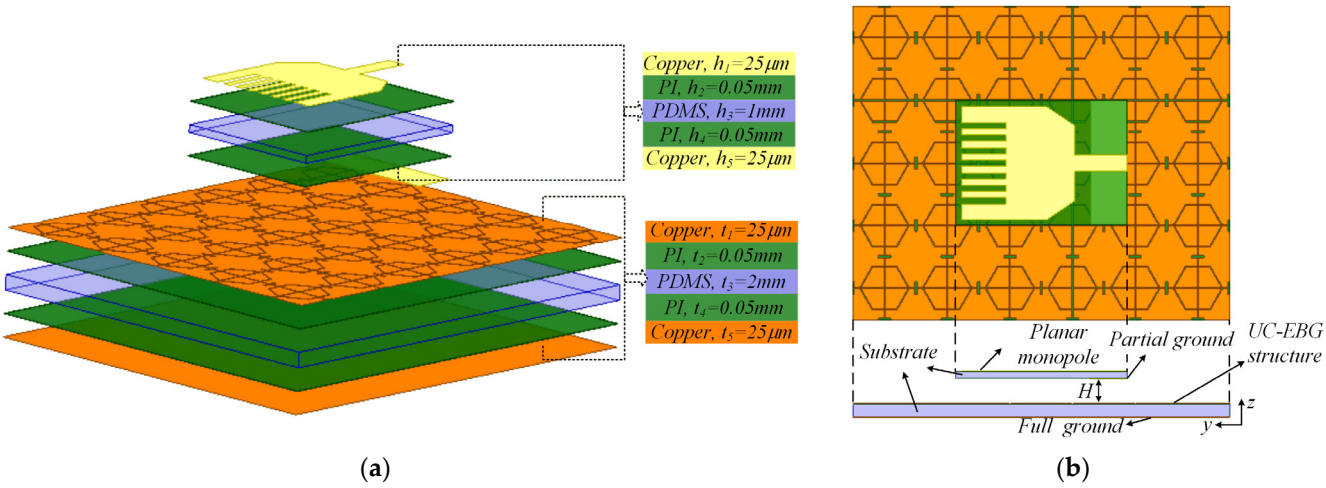

Figure 5. Configuration of the proposed monopole antenna with UC-EBG. (**a**) Layered graph. (**b**) Top view and side view.

Figure 6 illustrates the reflection coefficient of the monopole antenna with UC-EBG. As we can see, from 4.2 GHz to 7.5 GHz, the reflection coefficient is less than −10 dB.

Furtherly, the backward radiation is suppressed effectively, and the antenna directivity and gain are improved observably, which is proved in Figure 7.

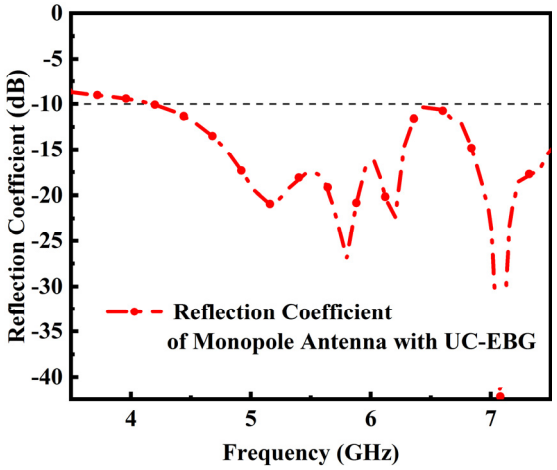

Figure 6. Reflection coefficient of the monopole antenna with UC-EBG.

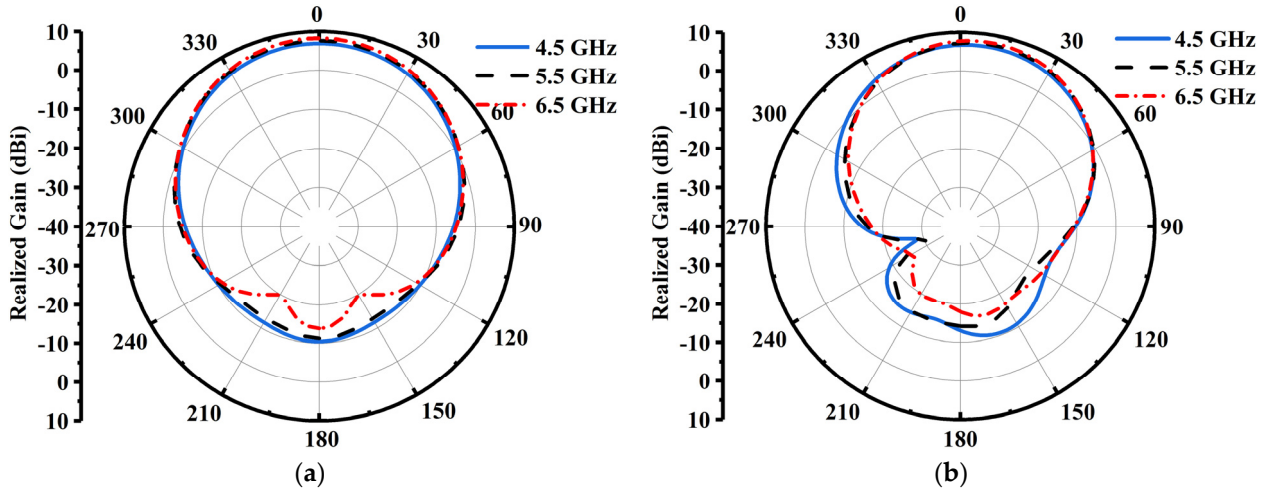

Figure 7. The radiation patterns of the monopole antenna with UC-EBG at different frequencies. (**a**) xoz plane. (**b**) yoz plane.

2.2. Antenna Performance on Human Body

To verify the antenna performance on the human body, the wearable antenna performance was simulated under on-body status, which is displayed in Figures 8 and 9. The three-dimensional model of the male of ANSYS HFSS was adopted to mimic real scenarios, which is depicted in Figure 10a. The particular human body model and the typical permittivity, conductivity and mass density values of human tissue have been reported in [27]. As plotted in Figure 8a,b, from 4.5–6.5 GHz, the reflection coefficient of the monopole with UC-EBG on the human body is less than −10 dB while the efficiency of the antenna element maintains over 80%. Figure 9 illustrates the radiation patterns of the monopole with UC-EBG, which show stability at different frequencies. The simulated results indicate that the antenna performance changes insignificantly between on-body and off-body status due to the isolation offered by the UC-EBG structure.

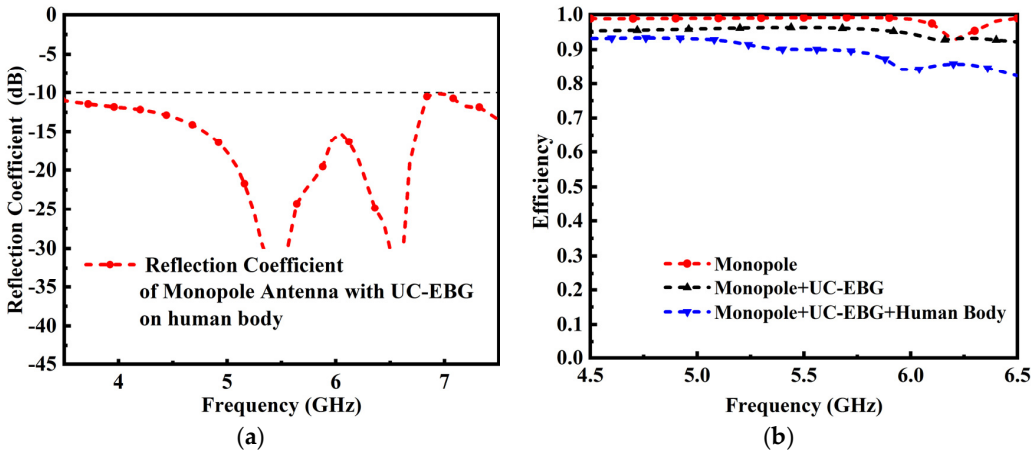

Figure 8. (**a**) Reflection coefficient of the monopole with UC-EBG on the human body. (**b**) The efficiency of the proposed monopole in different conditions.

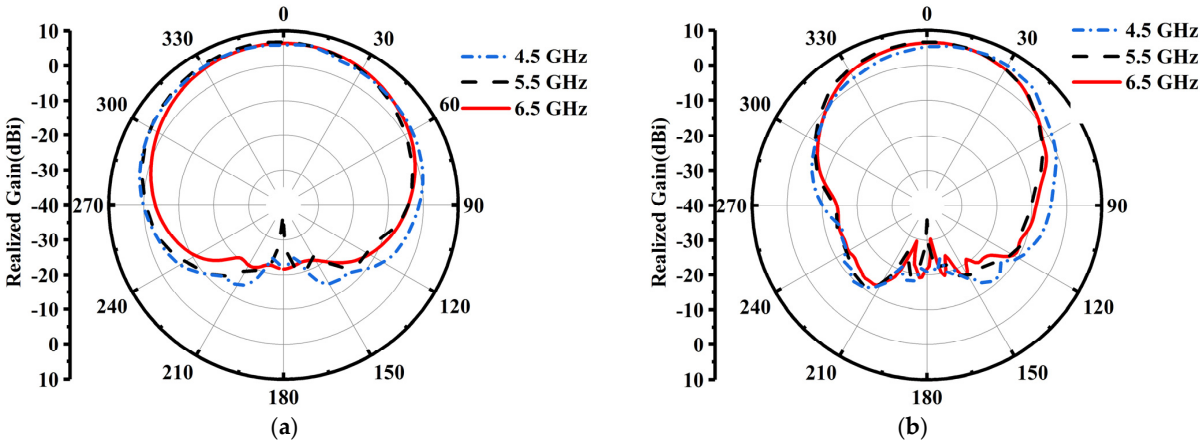

Figure 9. The (**a**) xoz plane radiation patterns and (**b**) yoz radiation patterns of the monopole with UC-EBG.

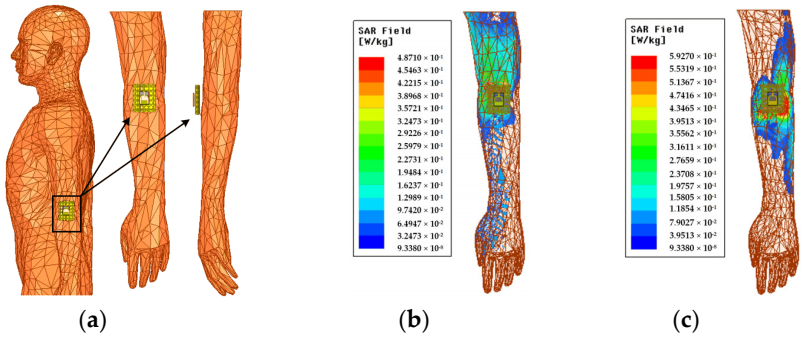

Figure 10. (**a**) The wearable antenna loaded on the voxel model. SAR simulation at (**b**) 4 GHz and (**c**) 6 GHz.

Considering the verification of human safety, we simulated the SAR value of the monopole antenna with UC-EBG when it is placed on the human body with the distance of 8 mm. Figure 10b,c plot the value of SAR for 1 g human tissue at 4 GHz and 6 GHz, respectively. The federal communications commission (FCC) stipulates that the SAR value cannot exceed 1.6 W/kg s for 1 g human tissue. As depicted in Figure 10, a maximum 1 g SAR value of 0.49 W/kg at 4 GHz and 1 g SAR value of 0.59 W/kg at 6 GHz are achieved, which is much lower than FCC standard, guaranteeing the safety for wearable application.

2.3. Antenna Array Design

To further meet the requirement of high directivity and high gain in wearable antenna design, while maintaining the advantage of wide operating band, a four-way power divider is utilized to parallelly feed the 4 monopole antenna elements. Combined with the UC-EBG structure, the wideband and high-gain wearable antenna array is achieved. As illustrated in Figure 11, the distance between adjacent elements is 40.77 mm, and the in-phase reflector consists of 17 × 7 UC-EBG units.

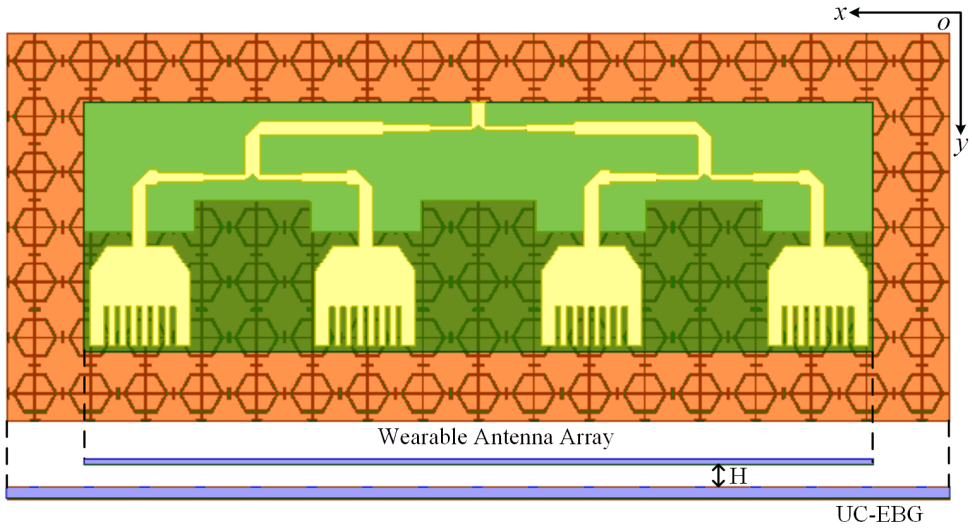

Figure 11. Configuration of the proposed wearable antenna array.

Figure 12a plots the reflection coefficient of the proposed wearable antenna array, which is less than −10 dB from 4.4 GHz to 7 GHz, covering the operating band 4.5–6.5 GHz. Figure 12b depicts the efficiency of the proposed antenna array, which is over 75% within the whole working band. The radiation patterns of the proposed wearable antenna array at different frequencies are displayed in Figure 13a–c. The realized gain and radiation efficiency are plotted in Figure 13d. Within the working frequency band from 4.5 GHz to 6.5 GHz, the realized gain ranges between 12.1–14.2 dBi with an average radiation efficiency of 82%. Moreover, the sidelobe level in the xoz-plane is less than −12 dB, and the cross polarization in the main radiation direction is less than −40 dB, which shows low cross polarization in both xoz-plane and yoz-plane. The impedance performance and radiation performance indicate that the proposed antenna can operate from 4.5 GHz to 6.5 GHz, while achieving high gain, wide working frequency and low cross polarization.

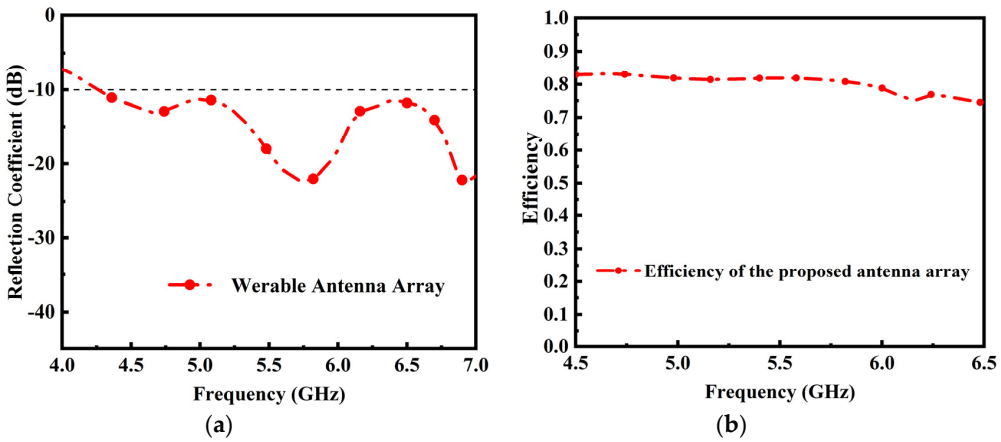

Figure 12. (**a**) Reflection coefficient of the proposed antenna array. (**b**) The efficiency of the proposed antenna array.

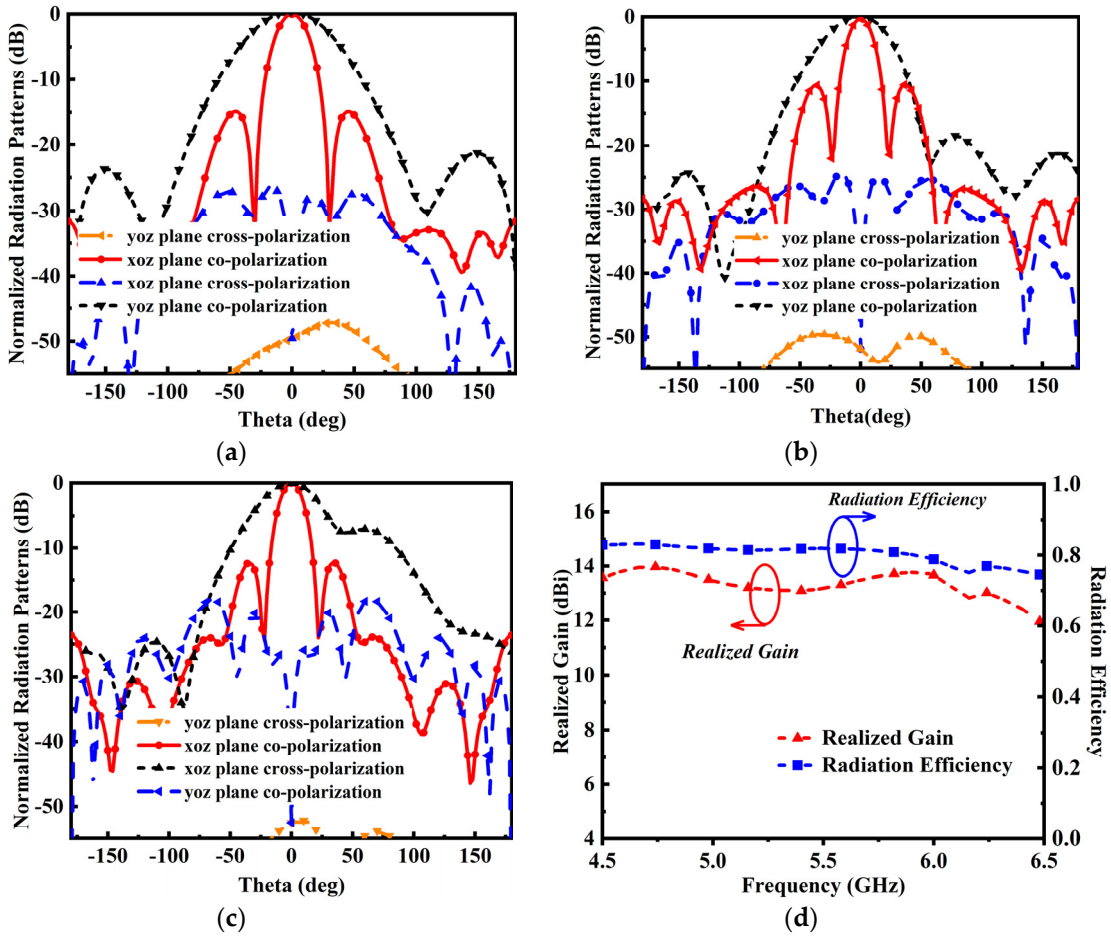

Figure 13. Normalized radiation patterns of the proposed wearable antenna array at (**a**) 4.5 GHz, (**b**) 5.5 GHz and (**c**) 6.5 GHz. (**d**) Realized gain and radiation efficiency of the antenna array.

3. Experimental Validation and Discussion

Prototypes of the proposed wideband and high-gain wearable antenna array were fabricated for experimental validation as displayed in Figure 14, which shows good flexibility. As depicted in Figure 15, the proposed wearable antenna array was measured in the anechoic chamber. Figure 16 plots the measured reflection coefficient. From 4.5–6.5 GHz, the reflection coefficient maintained less than −10 dB on different parts of the human body.

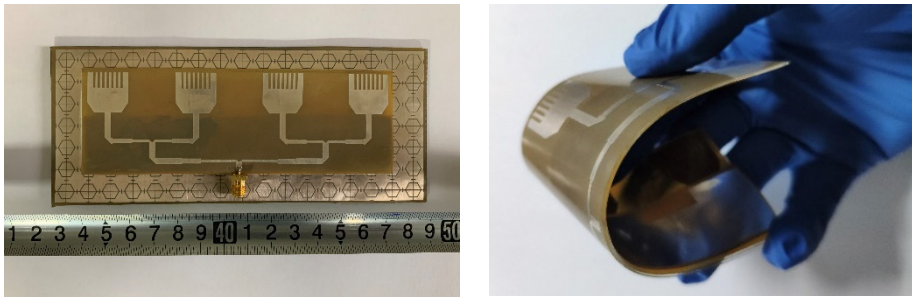

(**a**) (**b**)

Figure 14. The photographs of the proposed wearable antenna array in the (**a**) flat state and (**b**) bending state.

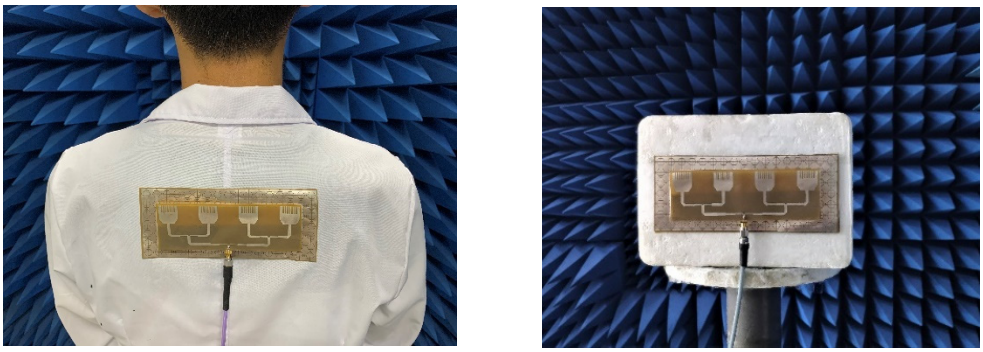

(**a**) (**b**)

Figure 15. The photograph of the (**a**) on-body and (**b**) off-body measurement environment.

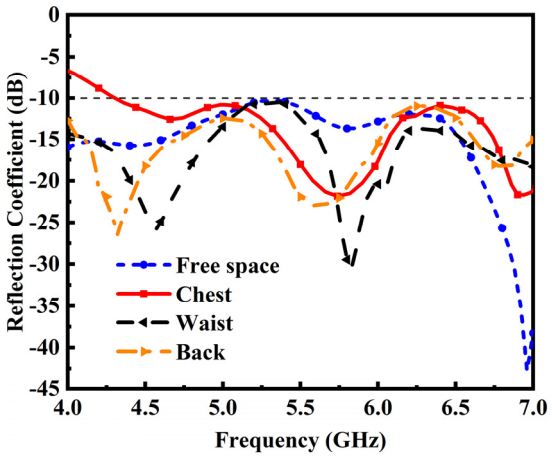

Figure 16. The measured reflection coefficients on different parts of the body.

The radiation patterns of the proposed antenna array were measured. Figure 17 presents the simulated and measured radiation patterns in the xoz plane and yoz plane at 4.5 GHz, 5.5 GHz and 6.5 GHz, and Figure 18 plots the comparison between the measured and simulated realized gain. Within the operating band, the measured realized gain ranges from 11.8–13.6 dBi with −35 dB measured cross polarization. The proposed wearable antenna array maintained stable measured radiation performance, which shows great agreement with simulated results.

Table 2 lists the comparison of the proposed antenna with other wearable antennas. It can be concluded that the proposed antenna array offers 36% relative bandwidth and 13.6 dBi realized gain, which provides a method to achieve wideband and high-gain wearable antenna with SAR suppression.

Table 2. Comparison of the wearable antenna array with other works.

Ref.	Structure	Operating Bandwidth (%)	Gain (dBi)	SAR (w/kg)
[24]	Microstrip	9%	6.0	0.29
[28]	Monopole & AMC	34%	6.12	0.56
[29]	Loop	7%	3.9	NA
[30]	Microstrip	5%	5.09	0.64
Our work	Monopole & EBG	36%	13.6	0.59

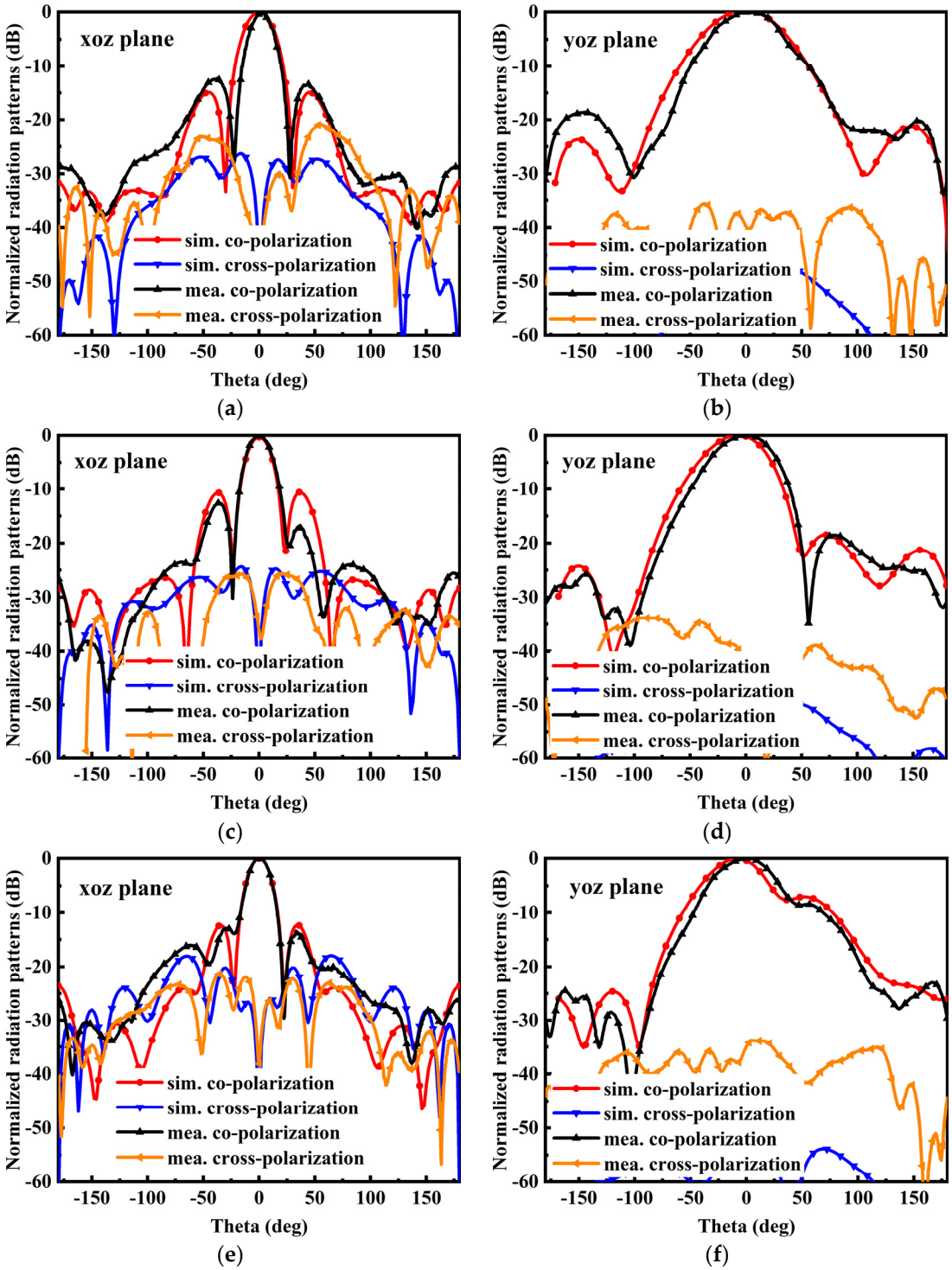

Figure 17. The measured and simulated normalized radiation patterns of the proposed wearable antenna array at (**a**,**b**) 4.5 GHz, (**c**,**d**) 5.5 GHz and (**e**,**f**) 6.5 GHz.

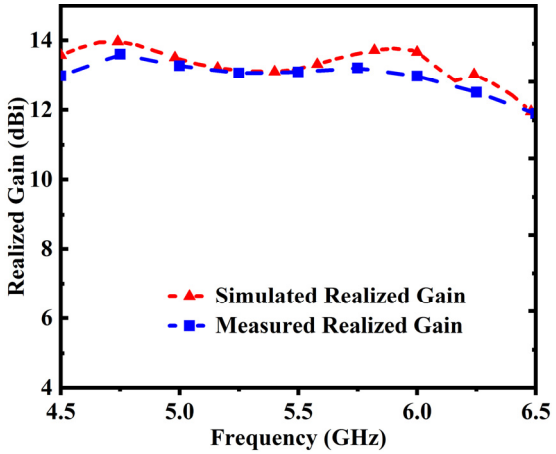

Figure 18. The measured and simulated realized gain.

4. Conclusions

A novel wideband and high-gain wearable antenna array with specific absorption rate suppression is proposed. Benefiting from the combination of wideband antenna elements and wideband UC-EBG in-phase reflector, the proposed wearable antenna array provides the operating band 4.5–6.5 GHz with the measured realized gain of 11.8–13.6 dBi, and the measured cross polarization is less than −35 dB. The proposed wideband and high-gain wearable antenna array offers some advantages in the wearable application.

Author Contributions: H.Z. put forward the concept (Conceptualization) and analyzed the proposed structure (Formal analysis). B.W. put forward the concept (Conceptualization) and coordinated the research (Project administration). P.Y. managed the simulation data (Data curation) and wrote the initial draft (Writing—original draft). W.L. analyzed the proposed structure (Formal analysis) and modified the original draft (Writing—review & editing). J.L. managed the simulation data (Data curation) and synthesized study data (Formal analysis). All authors have read and agreed to the published version of the manuscript.

Funding: This research was funded by the National Natural Science Foundation of China (NSFC) under projects No. 61771360, 62071357, 62171348, U19A2055, the Key Industry chain Project of Shaanxi Province No. 2018ZDCXL-GY-08-03-01, the Fundamental Research Funds for the Central Universities, the 111 Project of China.

Conflicts of Interest: The authors declare no conflict of interest.

References

1. Karaoguz, J. High-rate wireless personal area networks. *IEEE Commun. Mag.* **2001**, *39*, 96–102. [CrossRef]
2. Alqadami, A.S.M.; Bialkowski, K.S.; Mobashsher, A.T.; Abbosh, A.M. Wearable Electromagnetic Head Imaging System Using Flexible Wideband Antenna Array Based on Polymer Technology for Brain Stroke Diagnosis. *IEEE Trans. Biomed. Circuits Syst.* **2019**, *13*, 124–134. [CrossRef] [PubMed]
3. Yan, S.; Vandenbosch, G.A.E. Wearable antenna with tripolarization capability. In Proceedings of the 2017 International Workshop on Antenna Technology: Small Antennas, Innovative Structures, and Applications (iWAT), Athens, Greece, 1–3 March 2017; pp. 129–131.
4. Alqadami, A.S.M.; Nguyen-Trong, N.; Mohammed, B.; Stancombe, A.E.; Heitzmann, M.T.; Abbosh, A.M. Compact unidirectional conformal antenna based on flexible high-permittivity custom-made substrate for wearable wideband EM head imaging system. *IEEE Trans. Antennas Propag.* **2020**, *68*, 183–194. [CrossRef]
5. Zu, H.R.; Wu, B.; Zhang, Y.H.; Zhao, Y.T.; Song, R.G.; He, D.P. Circularly Polarized Wearable Antenna With Low Profile and Low Specific Absorption Rate Using Highly Conductive Graphene Film. *IEEE Antennas Wirel. Propag. Lett.* **2020**, *19*, 2354–2358.
6. Salvado, R.; Loss, C.; Gonçalves, R.; Pinho, P. Textile materials for the design of wearable antennas: A survey. *Sensors* **2012**, *12*, 15841–15857. [CrossRef]
7. Ali, S.M.; Sovuthy, C.; Imran, M.A.; Socheatra, S.; Abbasi, Q.H.; Abidin, Z.Z. Recent advances of wearable antennas in materials, fabrication methods, designs, and their applications: State-of-the-art. *Micromachines* **2020**, *11*, 888. [CrossRef]
8. Sanjeeva Reddy, B.R.; Darimireddy, N.K.; Park, C.-W.; Chehri, A. Performance of Reconfigurable Antenna Fabricated on Flexible and Nonflexible Materials for Band Switching Applications. *Energies* **2021**, *14*, 2553. [CrossRef]

9. Salonen, P.; Sydanheimo, L.; Keskilammi, M.; Kivikoski, M. A small planar inverted-F antenna for wearable applications. In Proceedings of the Third International Symposium on Wearable Computers, San Francisco, CA, USA, 18–19 October 1999; pp. 95–100.
10. Hamouda, Z.; Wojkiewicz, J.-L.; Pud, A.A.; Koné, L.; Belaabed, B.; Bergheul, S.; Lasri, T. Dual-Band Elliptical Planar Conductive Polymer Antenna Printed on a Flexible Substrate. *IEEE Trans. Antennas Propag.* **2015**, *63*, 5864–5867. [CrossRef]
11. Hu, B.; Gao, G.P.; He, L.L.; Cong, X.D.; Zhao, J.N. Bending and On-Arm Effects on a Wearable Antenna for 2.45 GHz Body Area Network. *IEEE Antennas Wirel. Propag. Lett.* **2016**, *15*, 378–381. [CrossRef]
12. Hamouda, Z.; Wojkiewicz, J.; Pud, A.A.; Koné, L.; Bergheul, S.; Lasri, T. Magnetodielectric Nanocomposite Polymer-Based Dual-Band Flexible Antenna for Wearable Applications. *IEEE Trans. Antennas Propag.* **2018**, *66*, 3271–3277. [CrossRef]
13. Lin, C.P.; Chang, C.H.; Cheng, Y.T.; Jou, C.F. Development of a Flexible SU-8/PDMS-Based Antenna. *IEEE Antennas Wirel. Propag. Lett.* **2011**, *10*, 1108–1111.
14. Mendes, C.; Peixeiro, C. A dual-mode single-band wearable microstrip antenna for body area networks. *IEEE Antennas Wirel. Propag. Lett.* **2017**, *16*, 3055–3058. [CrossRef]
15. Liu, X.Y.; Di, Y.H.; Liu, H.; Wu, Z.T.; Tentzeris, M.M. A Planar Windmill-Like Broadband Antenna Equipped with Artificial Magnetic Conductor for Off-Body Communications. *IEEE Antennas Wirel. Propag. Lett.* **2016**, *15*, 64–67. [CrossRef]
16. Agarwal, K.; Guo, Y.X.; Salam, B. Wearable AMC Backed Near-Endfire Antenna for On-Body Communications on Latex Substrate. *IEEE Trans. Compon. Packag. Manuf. Technol.* **2016**, *6*, 346–358. [CrossRef]
17. El Atrash, M.; Abdalla, M.A.; Elhennawy, H.M. A Wearable Dual-Band Low Profile High Gain Low SAR Antenna AMC-Backed for WBAN Applications. *IEEE Trans. Antennas Propag.* **2019**, *67*, 6378–6388. [CrossRef]
18. Raad, H.R.; Abbosh, A.I.; Al-Rizzo, H.M.; Rucker, D.G. Flexible and Compact AMC Based Antenna for Telemedicine Applications. *IEEE Trans. Antennas Propag.* **2013**, *61*, 524–531. [CrossRef]
19. Zhu, S.Z.; Langley, R. Dual-Band Wearable Textile Antenna on an EBG Substrate. *IEEE Trans. Antennas Propag.* **2009**, *57*, 926–935. [CrossRef]
20. Kim, S.; Ren, Y.J.; Lee, H.; Rida, A.; Nikolaou, S.; Tentzeris, M.M. Monopole Antenna With Inkjet-Printed EBG Array on Paper Substrate for Wearable Applications. *IEEE Antennas Wirel. Propag. Lett.* **2012**, *11*, 663–666. [CrossRef]
21. Ashyap, A.Y.I.; Abidin, Z.Z.; Dahlan, S.H.; Majid, H.A.; Shah, S.M.; Kamarudin, M.R.; Alomainy, A. Compact and Low-Profile Textile EBG-Based Antenna for Wearable Medical Applications. *IEEE Antennas Wirel. Propag. Lett.* **2017**, *16*, 2550–2553. [CrossRef]
22. Gao, G.P.; Hu, B.; Wang, S.F.; Yang, C. Wearable Circular Ring Slot Antenna With EBG Structure for Wireless Body Area Network. *IEEE Antennas Wirel. Propag. Lett.* **2018**, *17*, 434–437. [CrossRef]
23. Sambandam, P.; Kanagasabai, M.; Ramadoss, S.; Natarajan, R.; Alsath, M.G.N.; Shanmuganathan, S.; Sindhadevi, M.; Palaniswamy, S.K. Compact Monopole Antenna Backed With Fork-Slotted EBG for Wearable Applications. *IEEE Antennas Wirel. Propag. Lett.* **2020**, *19*, 228–232. [CrossRef]
24. Mao, C.X.; Vital, D.; Werner, D.H.; Wu, Y.H.; Bhardwaj, S. Dual-Polarized Embroidered Textile Armband Antenna Array With Omnidirectional Radiation for On-/Off-Body Wearable Applications. *IEEE Trans. Antennas Propag.* **2020**, *68*, 2575–2584. [CrossRef]
25. Fan, C.; Wu, B.; Hu, Y.; Zhao, Y.T.; Su, T. Millimeter-wave Pattern Reconfigurable Vivaldi Antenna Using Tunable Resistor Based on Graphene. *IEEE Trans. Antennas Propag.* **2020**, *68*, 4939–4943. [CrossRef]
26. Fan, C.; Wu, B.; Song, R.G.; Zhao, Y.T.; Zhang, Y.H.; He, D.P. Electromagnetic shielding and multi-beam radiation with high conductivity multilayer graphene film. *Carbon* **2019**, *155*, 506–513. [CrossRef]
27. Stuchly, M.A.; Stuchly, S.S. Dielectric properties of biological substances-tabulated. *J. Microw. Power* **1980**, *15*, 19–25. [CrossRef]
28. Alemaryeen, A.; Noghanian, S. On-Body Low-Profile Textile Antenna with Artificial Magnetic Conductor. *IEEE Trans. Antennas Propag.* **2019**, *67*, 3649–3656. [CrossRef]
29. Hu, X.M.; Yan, S.; Vandenbosch, G.A.E. Comsspact Circularly Polarized Wearable Button Antenna with Broadside Pattern for U-NII Worldwide Band Applications. *IEEE Trans. Antennas Propag.* **2019**, *67*, 1341–1345. [CrossRef]
30. Guan, C.-E.; Fujimoto, T. Design of a Wideband L-Shape Fed Microstrip Patch Antenna Backed by Conductor Plane for Medical Body Area Network. *Electronics* **2020**, *9*, 21. [CrossRef]